JOURNAL OF SOLID STATE CHEMISTRY **138,** 1–6 (1998)
ARTICLE NO. SC977690

TPR, ESR, and XPS Study of Cu^{2+} Ions in Sol–Gel-Derived TiO_2

G. Córdoba,* M. Viniegra,* J. L. G. Fierro,† J. Padilla,* and R. Arroyo*, [1]

*Departamento de Química, Universidad Autónoma Metropolitana-Iztapalapa, P.O. Box 55-534, 09340 México, D.F., Mexico; and
†Instituto de Catálisis y Petroleoquímica, CSIC, Campus UAM, Cantoblanco, 28049 Madrid, Spain

Received May 14, 1997; in revised form October 30, 1997; accepted October 31, 1997

Fine titanium(IV) oxide amorphous powders containing two different amounts of CuO were prepared by the sol–gel process. The samples were crystallized to anatase by heating. The reduction of $CuO–TiO_2$ samples was investigated by temperature-programmed reduction (TPR). Three types of signals were detected: Two of them are strong and were assigned to two different types of copper ions distributed on the surface. The third kind was a weak broad signal and was ascribed to the simultaneous reduction of titanium and a third type of copper ion incorporated into the TiO_2 network. This was confirmed by electron spin resonance measurements of the samples before and after programmed reductions at various temperatures selected from the TPR profiles. The results showed that the lowest reduction temperature is due to the existence of isolated copper ions distributed on the surface. The second TPR peak was due to a CuO phase with small particle size. These results were consistent with X-ray photoelectron spectroscopy studies, which showed two signals assigned to –Cu–O–Ti–O– and CuO species.

INTRODUCTION

Different methods are currently being used to obtain information on structural changes that occur during the phase transformations in solids prepared by the sol–gel process. These methods include nuclear magnetic resonance (1), Raman spectroscopy (2, 3), and X-ray diffraction (3, 4). However, frequently additional techniques are needed to characterize the chemical and structural evolution of the sol–gel solids, especially if other components are introduced along with the starting materials (5–8). During the preparation of doped materials by the sol–gel process, an inhomogeneous distribution of the dopant cations due to different factors can exist (5, 6). The differentiation of the various species present in the solid is important due to potential applications in optical (7), magnetic (9), electrical (10), and catalytic materials (11). In the present work, the distribution of copper ions in the mixed oxide $CuO–TiO_2$, prepared by the sol–gel method, was studied. The characterization of the materials was achieved mainly by temperature-programmed reduction (TPR), electron spin resonance (ESR), and X-ray photoelectron spectroscopy (XPS).

TPR is a relatively simple technique which was been used to characterize a variety of oxides. Peaks in the TPR profiles can be assigned to the reduction of a particular component (12). The ESR signal of Cu(II) ions incorporated into solids can provide information about the environment in which the paramagenetic centers are situated. Several ESR studies of Cu(II) ions in oxide glasses and zeolites have been made recently (6, 11, 13–17). The XPS technique is useful to determine the chemical structure of the surface. Information about the chemical composition and chemical bonding of the superficial species can be obtained by analyzing chemical shifts, satellites, and multiplet structure in the XPS spectra (8, 17–21).

EXPERIMENTAL

The sol–gel synthesis of $CuO–TiO_2$ samples with varying amounts of CuO (0, 5, and 10 mol%) was achieved by adding, with stirring, a solution of $Ti[OCH(CH_3)_2]_4$ (TIPT) diluted with 2-propanol [$TIPT:HOCH(CH_3)_2 = 1:2$ molar ratio] to a solution of $Cu(CH_3COO)_2 \cdot H_2O$ in ammonium hydroxide (28 wt% NH_3 in water) and 2-propanol [$HOCH(CH_3)_2:H_2O:NH_4OH = 2:1:0.33$ molar ratio]. Precipitation occurred in seconds. This mixture was stirred at room temperature for 20 min. After that, 3 mol of deionized water was added, and a major precipitation occurred. Stirring was continued for another 60 min. The resultant mixture was aged for 24 h, and the residual liquid (colorless) was then removed by decanting. Addition of acetate groups to TIPT was not investigated. The solids were converted to xerogels by heating at 353 K in a drying oven for 24 h and later divided into aliquots which were treated at a heating rate of 5 K/min in a furnace at 623 and 698 K for 72 h in air. The samples containing 5 and 10 mol% treated at 623 K will hereafter be referred to as

[1] To whom correspondence should be addressed.

0022-4596/98 $25.00

TCuO5-1 and TCuO10-1, and those treated at 698 K as TCuO5-2 and TCuO10-2, respectively.

Thermogravimetric analysis (TGA) and differential thermal analysis (DTA) measurements were performed with a Shimadzu DT-30 instrument to investigate the thermal behavior of the xerogels; an open aluminium basket in a dry air atmosphere and a heating rate of 20 K/min were used for these experiments. X-ray diffraction (XRD) patterns were obtained on a Siemens D-500 diffractometer (CuK_α radiation, $\lambda = 0.1543$ nm). Bragg angles ranging from 5° to 70° were scanned at a rate of 1°/min. The surface area of the dried samples was measured using commercial BET measurement equipment (ISRI-RIG-100).

TPR of samples was carried out using 5 mol% hydrogen in argon as a reducing gas. The temperature of the sample was controlled with a programmable controller (Omega CN-2010) at a heating rate of 5 K/min. The gas flow rate was adjusted by mass flow controllers to 60 mL/min and the hydrogen consumption was followed with a thermal conductivity detector (TCD). The reactor used for TPR was made of an 8-mm-i.d. quartz tube and the sample (100 mg) was mounted on a quartz plate. The outlet of the TPR cell was connected to a quartz column packed with molecular sieve 3 Å to remove water produced from the reduction. The samples reduced at different temperatures utilized for ESR experiments were prepared in the reactor and then transferred to the quartz tube without exposing them to air.

ESR measurement were made on a Bruker ER-200 D-SRC spectrometer working at the X-band frequency and 100-kHz field modulation. The spectra were recorded at 291 and 77 K. The finely powdered sample, contained in a quartz tube, was introduced into the resonance cavity. Microwave frequency was measured with a frequency counter. The magnetic field was measured with a gaussmeter (Bruker ER035 M). The simulation of the ESR spectra was performed with the program "EPR: A Modelling Approach", written by Frank Neese of the University of Konstanz, Germany. The g and hyperfine splitting values used in this work are taken from the simulated spectra.

X-ray photoelectron spectra were acquired with a VG ESCALAB 200R spectrometer equipped with a MgK_α 120-W X-ray source ($h\upsilon = 1253.6$ eV). Both calcined and H_2-reduced samples were analyzed by XPS. The samples were pressed into small aluminum cylinders and then mounted on a sample rod placed in a pretreatment chamber and outgassed at room temperature or prereduced in H_2 at 523 and 623 K for 1 h prior to being transferred to the analysis chamber. The pressure in the ion-pumped analysis chamber was below 3×10^{-9} Torr during data acquisition. The spectra were collected for 20–90 min, depending on the peak intensities, at a pass energy of 10 eV. The intensities were estimated by calculating the integral of each peak after smoothing and subtraction of the S-shaped background and fitting the experimental curve to a combination of Gaussian and Lorentzian lines of variable proportion. All binding energies (BE) were referenced to the adventitious C 1s line at 284.9 eV. This reference gave BE values within an accuracy of $\pm$ 0.1 eV.

RESULTS AND DISCUSSION

The calcination temperatures were selected based on the results of the TGA and DTA of the xerogels. These results showed a weight loss from room temperature up to approximately 600 K together with an endothermic peak (about 360 K) and an asymmetric exothermic peak (about 525 K). The former was assigned to the loss of 2-propanol and water (22) and to the decomposition of amine copper complexes (23). The exothermic peak, whose relative intensity depends on the copper content, was due to the decomposition of acetate groups, which is strongly exothermic (24). Finally, the TGA did not show additional weight losses, and the DTA showed a sharp exothermic peak at 750 K, which was assigned to a phase change of TiO_2 (25).

The XRD pattern obtained from the xerogels showed that these are amorphous. The XRD patterns of the TiO_2, TCuO5-2, and TCuO10-2 samples are shown in Fig. 1.

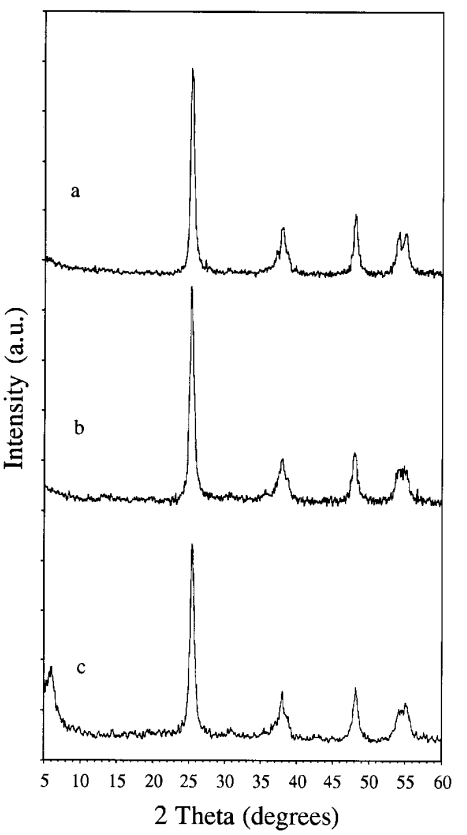

FIG. 1. X-ray diffraction patterns of samples treated at 698 K: (a) TiO_2, (b) TCuO5, and (c) TCuO10.

TABLE 1
Specific Surface Area Results

Thermal treatment (K)	Sample	Surface area (m^2/g)
623	TiO_2	44
	TCuO5	56
	TCuO10	90
698	TiO_2	21
	TCuO5	40
	TCuO10	61

These patterns present broad peaks due to anatase-type TiO_2, and no reflection is observed at $2\theta = 35.5^\circ$ corresponding to the most intense reflection of tenorite CuO; this means that if part of the copper exists in the form of CuO clusters, these are not large enough to be detected by XRD (26). This behavior suggests that the sol–gel method stabilizes the CuO phase in a highly dispersed state. The samples treated at 623 K showed similar results. The BET surface areas (Table 1) decreased with a rise in calcination temperature and increased with the addition of copper. This latter fact indicates that copper ions were effectively introduced into the TiO_2 network.

The TPR analysis for the samples treated at 623 and 698 K are shown in Figs. 2 and 3, respectively. It can be seen that in the samples without copper a small and very broad signal is present between 673 and 1023 K. This signal is related to the reduction of TiO_2 exclusively. In addition to the broad signal shifted to lower temperature, the samples containing copper show peaks at 425 and 448 K; the intensity of these peaks increases with the amount of copper. The peak at 425 K is assigned to the reduction of isolated superficial copper ions, and the other peak to the reduction of CuO particles. The shift in the reduction temperature of TiO_2 in these samples can be explained by the presence of Cu^0 clusters (formed after reduction of CuO particles) that may catalyze the reduction of Ti^{4+} (27).

Thermal treatment of samples at increasing temperatures produces a change in the ESR spectra due to the appearance of various copper species; these spectra (shown in Fig. 4) are anisotropic and have hyperfine splitting (HFS) features for different copper sites. The ESR spectrum (Fig. 4a) for the xerogel exhibits a pronounced peak at $g_\perp = 2.095$ and a poorly resolved quadruplet at $g_\parallel = 2.305$ arising from parallel hyperfine splitting. Such spectral features are characteristic of d^9 ions in axially distorted octahedral sites

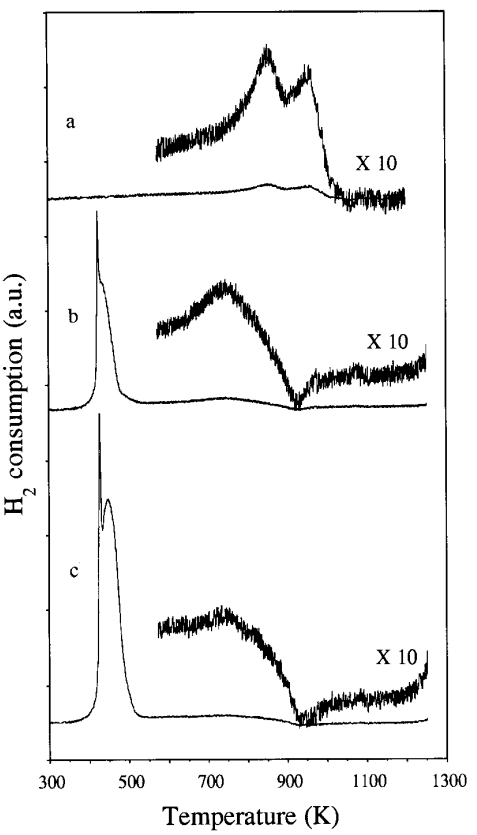

FIG. 2. Temperature-programmed reduction profiles of samples treated at 623 K [$m = 0.100$ g, gas = H_2/Ar (5 mol%), flow = 60 mL/min, ramp = 5K/min]: (a) TiO_2, (b) TCuO5, and (c) TCuO10.

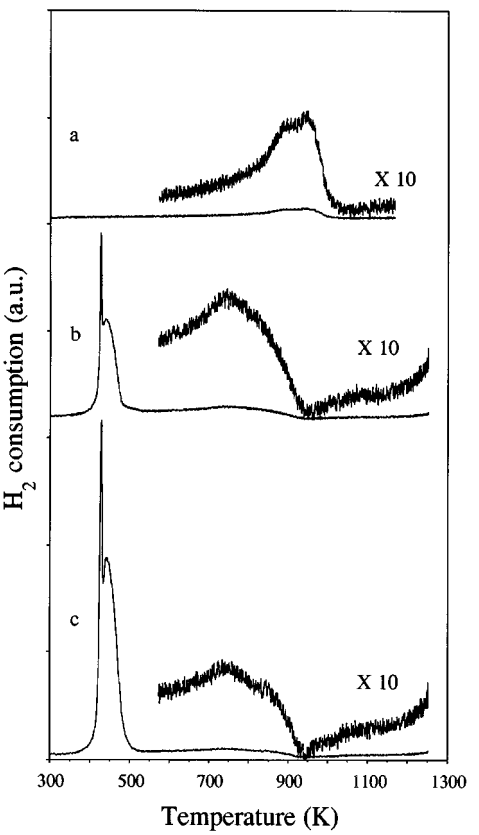

FIG. 3. Temperature-programmed reduction profiles of samples treated at 698 K [$m = 0.100$ g, gas = H_2/Ar (5 mol%), flow = 60 mL/min, ramp = 5K/min]: (a) TiO_2, (b) TCuO5, and (c) TCuO10.

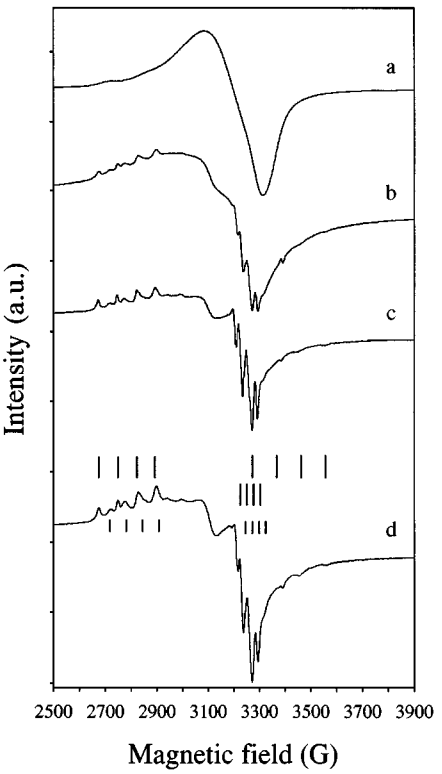

FIG. 4. ESR spectra at 77 K of TCuO5 and TCuO10: (a) xerogel, (b) TCuO5 treated at 623 K, (c) TCuO5 treated at 698 K, and (d) TCuO10 treated at 698 K. The large lines shown in (d) indicate the HFS assigned to copper ions incorporated into the TiO_2 network, and the short lines the HFS due to isolated superficial copper ions.

present in glassy systems (6, 8, 11, 13, 14). When the sample is heated, the spectra (Figs. 4b and 4c) differ significantly from that of the corresponding xerogel. Instead of broad signals, the spectra show well-resolved HFS lines for two different types of copper ions. A more defined spectrum is observed when the sample is heated at 698 K. The amount of copper does not affect the HFS as can be seen in Fig. 4d, which shows the spectrum of TCuO10-2. The computer-simulated spectrum for TCuO5-2 indicates the existence of two copper species in sites with well-defined spin-Hamiltonian parameters and another species that does not show HFS.

The spin-Hamiltonian parameters determined are shown in Table 2. TCuO5-2 unreduced sample shows three components. The following assignments are based on the combination of the ESR and programmed reductions (vide infra). The component with no resolved HFS is assigned to copper ions in CuO of small particle size on the TiO_2 surface (17), as supported by XRD data. The dipolar broadening of ESR lines did not permit the observation of HFS components for g (6, 11). For the second component, the spin-Hamiltonian parameters correspond to copper ions that remain isolated on the TiO_2 surface even after thermal treatment. The $g_\parallel$ and $g_\perp$ values are characteristic of an axially distorted octahedral site (13–16). The last component shows g values which correspond to copper ions present in an orthorhombic symmetry. We propose that such ions are incorporated into the TiO_2 network. The introduction of copper ions into the network produces an oxygen deficiency in the solid for the charge compensation (30).

The precise differentiation between these sites was possible by measuring the ESR spectrum of TCuO5-2 reduced in a programmed manner. The ESR spectra of the samples partially and totally reduced are shown in Fig. 5. As can be seen, the signal assigned to isolated superficial ions disappears when the reduction temperature is 510 K (Fig. 5c), as was observed in the TPR profile. When the reduction temperature is 573 K (Fig. 5d), the signal due to the clustered ions practically disappears and a new signal at $g = 2.002$ appears. This ESR signal, which is not present for reduction temperatures of 673 K or greater, is due to the conduction electrons that are present only in small nanocrystallites (7 nm or smaller) (28). This result is currently being studied. For reduction at 623 K (Fig. 5e) the spectrum changes; only one type of copper (incorporated into the network) is observed, and a signal due to Ti^{3+} arises with $g_\parallel = 1.89$ and $g_\perp = 1.96$ (29). The signal at $g = 2.002$ is still present. The spectrum of the sample reduced at 673 K (Fig. 5f) shows the signals assigned to incorporated copper ions and Ti^{3+}. Finally, when the sample is reduced at 1173 K, the signal of Ti^{3+} with $g_\parallel = 1.935$ and $g_\perp = 1.965$ is observed (Fig. 5g).

The spectral parameters obtained by XPS for samples treated at 698 K are summarized in Table 3. The BE for Ti

TABLE 2
Spin-Hamiltonian Parameters of ESR Spectra

Sample TCuO5-2 reduced at (K)	Assignment	g_x	g_y	g_z	A_x^a	A_y	A_z
Unreduced	Cu^{2+} in clusters			2.081			2.335
	Isolated surface Cu^{2+}			2.095		77	2.400
	Cu^{2+} incorporated into TiO_2	1.985	2.075	2.420	305	70	255
426	Cu^{2+} in clusters			2.078			2.340
	Isolated surface Cu^{2+}			2.079		82	2.400
	Cu^{2+} incorporated into TiO_2	1.985	2.085	2.430	250	75	260
510	Cu^{2+} in clusters			2.080			2.360
	Cu^{2+} incorporated into TiO_2	2.015	2.070	2.431	270	80	260
573	Cu^{2+} in clusters			2.081			2.356
	Cu^{2+} incorporated into TiO_2	1.986	2.086	2.470	245	85	250
	Conduction electrons			2.002			2.002
623	Cu^{2+} incorporated into TiO_2	1.985	2.087	2.430	265	80	260
	Conduction electrons			2.002			2.002
	Ti^{3+}			1.951		25	1.890
673	Cu^{2+} incorporated into TiO_2	1.985	2.089	2.426	265	82	250
	Ti^{3+}			1.940		50	1.890
1173	Ti^{3+}			1.965		21	1.935

[a] Units of A are megahertz.

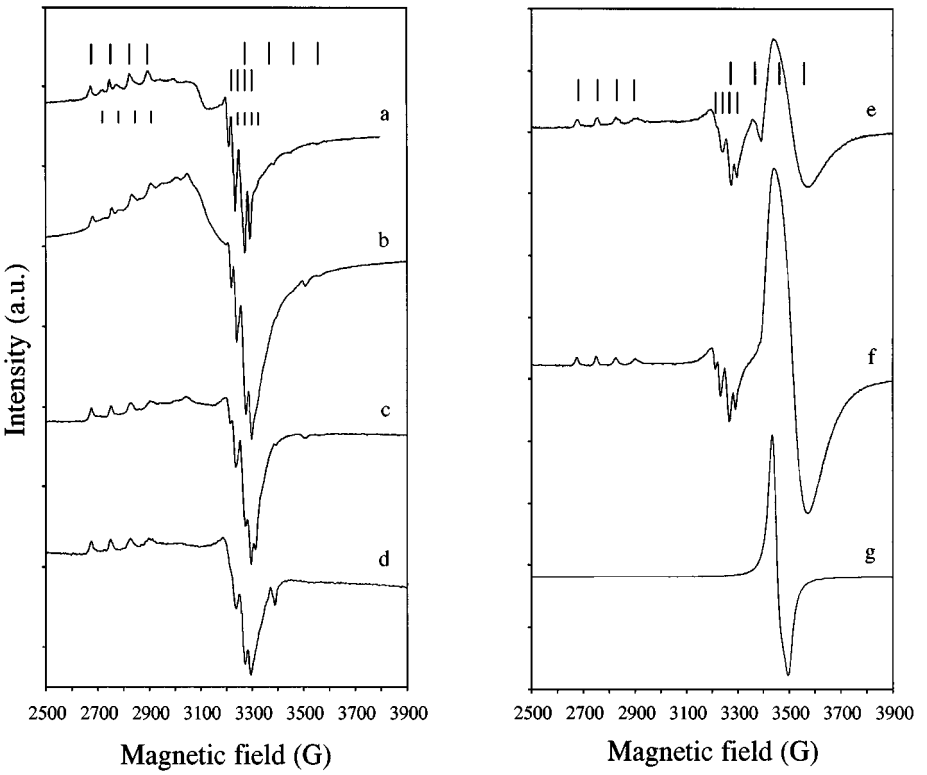

FIG. 5. ESR spectra at 77 K of TCuO5 treated at 698 K: (a) unreduced, (b) reduced at 426 K, (c) reduced at 510 K, (d) reduced at 573 K, (e) reduced at 623 K, (f) reduced at 673 K, and (g) reduced at 1173 K. The lines shown in (a) and (e) correspond to (long lines) HFS due to copper ions incorporated into the TiO_2 network, and (short lines) superficial isolated copper ions.

$2p_{3/2}$ and O 1*s* are typical for TiO_2 (21). The XPS Cu $2p_{3/2}$ core-level spectra of TCuO5-2 and TCuO10-2 samples are shown in Fig. 6.

TABLE 3
Binding Energies (eV) of Core Electrons and Surface (XPS) Atomic Ratios for Samples Treated at 698 K

Sample	Treatment	Ti $2p_{3/2}$	O 1*s*	Cu $2p_{3/2}$	Cu/Ti at
TiO_2	vacuum		529.9(83)		
		458.5	531.6(17)		
TiO_2	H_2 at 523 K		529.9(80)		
		458.5	531.4(20)		
TiO_2	H_2 at 623 K		529.9(85)		
		458.5	531.5(15)		
TCuO5	vacuum		529.8(87)	932.6(47)	
		458.5	531.4(13)	934.7(27)	0.232
TCuO5	H_2 at 523 K		529.9(88)	932.6(85)	
		458.5	531.0(12)	934.5(15)	0.221
TCuO5	H_2 at 623 K		529.9(87)		
		458.5	531.1(13)	932.4	0.089
TCuO10	vacuum		530.0(86)	632.6(19)	
		458.5	531.6(14)	634.8(45)	0.385
TCuO10	H_2 at 523 K		529.9(86)	932.4(92)	
		458.5	531.3(14)	933.6(8)	0.150
TCuO10	H_2 at 623 K		529.9(86)		
		458.5	531.3(14)	932.2	0.106

The TCuO5-2 and TCuO10-2 samples outgassed under vacuum (Figs. 6a and 6b) present two contributions to the Cu $2p_{3/2}$ peak: one near 933 eV and another near 935 eV associated with the CuO and –Cu–O–Ti–O– species, respectively. These signals are accompanied by the typical satellite peaks characteristic of Cu(II). The XPS spectra after reduction at 523 K (Figs. 6c and 6d) show that the satellite peaks practically disappear; in addition, the peak intensity assigned to CuO decreases and its position is shifted to 933.6 eV. The existence of CuO is also observed by ESR. When the samples are reduced at 623 K, the spectra do not show the satellite peaks, indicating the complete reduction of copper, and the BE observed corresponds to bulk copper (20); the decrease in the I_{Cu}/I_{Ti} ratio is most likely due to the aggregation of copper into small particles. These spectra show the reduction of surface copper species, and therefore it is not possible to observe the copper species entrapped in the bulk.

CONCLUSIONS

$CuO–TiO_2$ mixed oxides have been prepared by the sol–gel technique. From the present study, the following conclusions can be made. It is shown that copper(II) ions

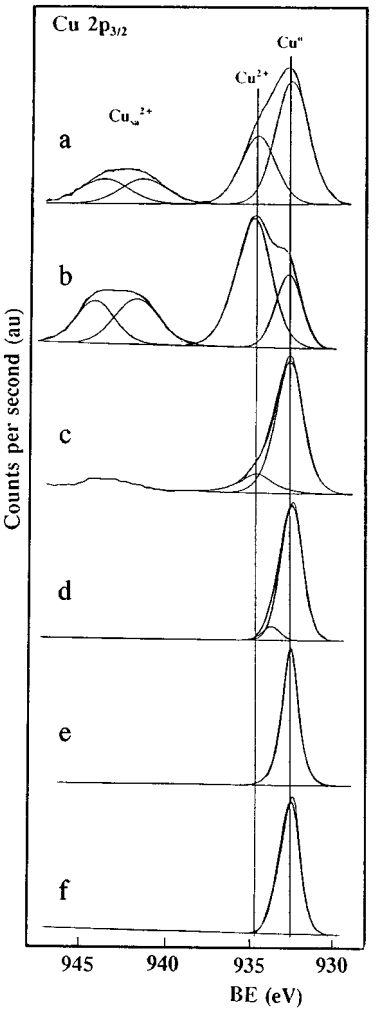

FIG. 6. Cu $2p_{3/2}$ XPS spectra of samples treated at 698 K: (a) TCuO5, vacuum; (b) TCuO10, vacuum; (c) TCuO5, H_2 reduced at 523 K; (d) TCuO10, H_2 reduced at 523 K; (e) TCuO5, H_2 reduced at 623 K; and (f) TCuO10, H_2 reduced at 523 K.

exist in three different environments in the samples. Isolated copper(II) ions incorporated into the titania network were detected by ESR spectroscopy, while two different copper(II) superficial species–one isolated on the titania surface and the other forming highly dispersed small CuO aggregates–were observed by TPR, ESR, and XPS. In addition, in spite of the high copper content (5 and 10 mol%) in the samples, they show a similar pattern in the ESR spectra, suggesting that the copper(II) ions do not show dipolar effects even at such a high molar percentage, which demonstrates the validity of this method of synthesis to obtain highly dispersed particles.

ACKNOWLEDGMENTS

The authors thank the Consejo Nacional de Ciencia y Tecnología (Projects 400200-5-3750E and 400200-5-1410PE) for financial support.

REFERENCES

1. K. Tadanaga, S. Ito, T. Minami, and N. Tohge, *J. Non-Cryst. Solids* **201,** 231 (1996).
2. E. Haro, S. Vargas, R. Arroyo, R. Rodríguez, and R. Diamant, *MRS Bull.* **31,** 329 (1996).
3. D. Bersani, P. P. Lottici, A. Montenero, S. Pigoni, and G. Gnappi, *J. Non-Cryst. Solids* **192&193,** 490 (1995).
4. Y. Kanno, *J. Mater. Res.* **9,** 2323 (1994).
5. G. De, A. Licciuli, and M. Nacucchi, *J. Non-Cryst. Solids* **201,** 153 (1996).
6. A. Shames, O. Lev, and B. I. Kuyavskaya, *J. Non-Cryst. Solids* **163,** 105 (1993).
7. G. De, M. Epifani, and A. Licciulli, *J. Non-Cryst. Solids* **201,** 250 (1996).
8. G. Córdoba, R. Arroyo, J. L. G. Fierro, and M. Viniegra, *J. Solid State Chem.* **123,** 93 (1996).
9. I. M. L. Billas, W. A. de Heer, and A. Chatelain, *J. Non-Cryst. Solids* **179,** 316 (1994).
10. T. K. Kundu and D. Chakravorty, *J. Mater. Res.* **9,** 2480 (1994).
11. J. Yan, A. M. Buckley, and M. Greenblatt, *J. Non-Cryst. Solids* **180,** 180 (1995).
12. N. K. Nag, D. Fraenkel, J. A. Moulijn, and B. C. Gates, *J. Catal.* **66,** 162 (1980).
13. B. Sreedhar, Ch. Sumalatha, and K. Kojima, *J. Non-Cryst. Solids* **192&193,** 203 (1995).
14. M. Shareefuddin, M. Jamal, and M. N. Chary, *J. Non-Cryst. Solids* **201,** 95 (1996).
15. T. Tanabe, T. Iijima, A. Koiwai, J. Mizuno, K. Yokota, and A. Isogai, *Appl. Catal. B* **6,** 145 (1995).
16. G. D. Lei, B. J. Adelman, J. Sárkány, and W. M. H. Sachtler, *Appl. Catal. B* **5,** 245 (1995).
17. O.V. Komova, L. T. Tzykoza, A. V. Simakov, A. V. Ushakov, V. A. Bolshov, G.B. Barannik, and Z. R. Ismagilov, *React. Kinet. Catal. Lett.* **52,** 129 (1994).
18. B. V. R. Chowdari and P. P. Kumari, *J. Non-Cryst. Solids* **197,** 31 (1996).
19. T. Tsuchida and H. Takahashi, *J. Mater. Res.* **9,** 2919 (1994).
20. X. Xu, J. W. He, and D. W. Goodman, *Surf. Sci.* **284,** 103 (1993).
21. H. Shin, R. J. Collins, M. R. De Guire, A. H. Heuer, and C. N. Sukenik, *J. Mater. Res.* **10,** 699 (1995).
22. Z. Congshen, H. Lisong, G. Fuxi, and J. Zhonghong, *J. Non-Cryst. Solids* **63,** 105 (1984).
23. M. Shimokawabe, H. Asakawa, and N. Takezawa, *Appl. Catal.* **59,** 45 (1990).
24. S. Doeuff, M. Henry, and C. Sanchez, "Better Ceramics through Chemistry II" (C. J. Brinker *et al.*, Eds.), p. 653. Elsevier, New York, 1986.
25. I. Manzini, G. Antonioli, D. Bersani, P. P. Lottici, G. Gnappi, and A. Montenero, *J. Non-Cryst. Solids* **192&193,** 519 (1995).
26. B. Coq, D. Tachon, F. Figuéras, G. Mabilon, and M. Prigent, *Appl. Catal. B* **6,** 271 (1995).
27. S. Yuan, P. Mériaudeau, and V. Perrichon, *Appl. Catal. B* **3,** 319 (1994).
28. X. Li and A. Vannice, *J. Catal.* **151,** 87 (1995).
29. L. Bonneviot and L. Hakker, *J. Catal.* **113,** 96 (1988).
30. R. Rodríguez, S. Vargas, R. Arroyo, R. Montiel, and E. Haro, *J. Mater. Res.* **12,** 439 (1997).